

# Synthesis of Functionalizable Boron-Containing $\pi$ -Electron Materials that Incorporate Formally Aromatic Fused Borepin Rings\*\*

Anthony Caruso, Jr., Maxime A. Siegler, and John D. Tovar\*

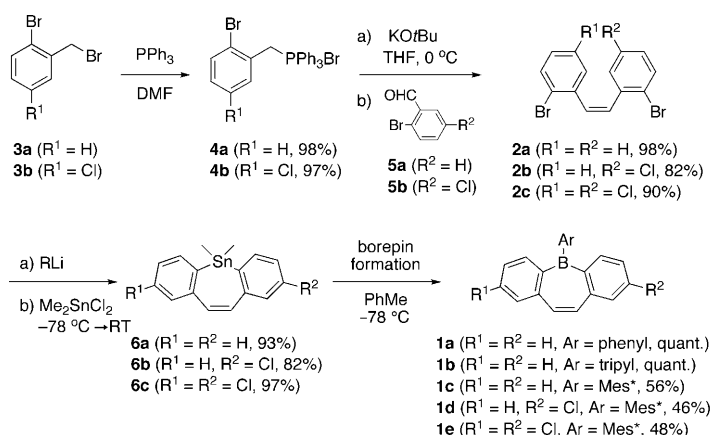
In memory of Eugene E. van Tamelen

Boron-containing  $\pi$ -electron systems have emerged as exciting subjects in contemporary organic materials chemistry.<sup>[1–7]</sup> The strong Lewis acidity of tricoordinate boron has been utilized for the detection of biologically or environmentally relevant anions.<sup>[8,9]</sup> Anionic and neutral boron heteroaromatic molecules are important  $\pi$ -donor ligands for organometallics,<sup>[10–12]</sup> and the aromaticity of boron-containing molecules has inspired substantial experimental and theoretical investigations,<sup>[13–16]</sup> thus suggesting that the heteroaromaticity of boron will play a key role in other areas where polarization may need to distort  $\pi$ -electron frameworks, such as during operation in electronic devices. The vast majority of boron-based  $\pi$ -electron materials was built with main-chain<sup>[17]</sup> or lateral<sup>[6,18,19]</sup> tricoordinate boron substitution or from locally antiaromatic four- $\pi$ -electron fragments such as the borole nucleus within 9-borafluorene.<sup>[20]</sup> Herein, we present the syntheses and characterization of polycyclic aromatic molecules built around the neutral and formally aromatic six- $\pi$ -electron borepin ring system that is structurally poised for synthetic elaboration into complex molecular structures.

The dibenzo[*b,f*]borepin (DBB) framework continues to attract substantial attention.<sup>[21,22]</sup> Van Tamelen et al. reported the first isolation of DBB as its ethanolamine adduct,<sup>[23]</sup> and Piers and co-workers very recently reported a *B*-mesityl DBB that slowly oxidized under ambient conditions.<sup>[24]</sup> Theoretical studies have revealed planarity throughout the *B*-H DBB; thus planarity was attractive to us as a means to enhance  $\pi$ -electron delocalization,<sup>[13]</sup> and nucleus-independent chemical shift (NICS) values reveal a weak degree of aromatic character within the borepin ring of benzo-annelated molecules.<sup>[14]</sup> However, no synthetic routes for robust and stable tricoordi-

nate borepins that could be tailored into complex  $\pi$ -electron systems have been reported to date.

The synthesis of the parent compound DBB **1a** is shown in Scheme 1. The stilbene precursor **2a** was constructed by a Wittig-type process using reactants derived from  $\alpha$ -bromo-*o*-



**Scheme 1.** Synthesis of dibenzo[*b,f*]borepins. Conditions for lithiation: **6a**: *s*BuLi, THF; **6b,c**: *n*BuLi, TMEDA, Et<sub>2</sub>O. Reagents for borepin formation: **1a**: PhBCl<sub>2</sub>; **1b**: a) BCl<sub>3</sub>, b) triptyl-SnBu<sub>3</sub>; **1c–e**: a) BCl<sub>3</sub>; b) Mes\*Li, RT. Yields for **1a** and **1b** determined by NMR spectroscopy. TMEDA = *N,N,N',N'*-tetramethylethane-1,2-diamine.

bromotoluene **3a**: radical halogenation and standard Arbusov reaction resulted in the phosphonium salt **4a**, while oxidation with *N*-methylmorpholine-*N*-oxide (NMO) furnished the requisite aldehyde **5a**. The desired *cis* product **2a** was dominant (> 90%) and was readily purified.<sup>[25]</sup> Stannocyclization was carried out by trapping the in situ generated dilithio species of **2a** with dimethyltin dichloride. Tin–boron exchange between **6a** and PhBCl<sub>2</sub> resulted in the *B*-phenyl DBB **1a**; both **1a** and even *B*-tripyl (2,4,6-triisopropylphenyl) DBBs **1b** rapidly decomposed under ambient conditions and were handled in a glovebox. Tri(*tert*-butylphenyl) (“super mesityl”, Mes\*) *B*-substituents rendered the resulting **1c** framework stable and sufficiently soluble to allow manipulation and chromatography under ambient conditions.<sup>[26]</sup>

The bulkier *B*-Mes\* substituent of **1c** slightly disturbed the  $\pi$ -conjugation, as indicated by the 14 nm blue shift of the lowest-energy UV/Vis features compared to those of **1a**, although the spectra remain qualitatively similar in terms of relative oscillator strengths.<sup>[27]</sup> Otherwise, the spectroscopic and electrochemical properties of DBB **1c** were comparable to those of the *B*-mesityl DBB frameworks reported inde-

[\*] A. Caruso, Jr., M. A. Siegler, Prof. J. D. Tovar  
Department of Chemistry  
Department of Materials Science and Engineering  
Johns Hopkins University  
3400 North Charles Street (NCB 316), Baltimore, MD 21218 (USA)  
Fax: (+1) 410-516-7044  
E-mail: tovar@jhu.edu  
Homepage: <http://www.jhu.edu/~chem/tovar/index.html>

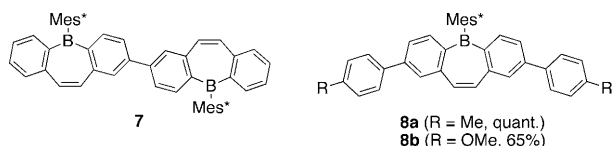
[\*\*] We thank Johns Hopkins University and the Petroleum Research Fund (administered by the American Chemical Society) for financial support. Prof. John Reynolds (University of Florida) provided helpful suggestions regarding the Ni-catalyzed homocoupling.

Supporting information for this article is available on the WWW under <http://dx.doi.org/10.1002/ange.201000411>.

pendently by Piers and co-workers.<sup>[24]</sup> However, the bulk of the Mes\* substituent shielded the boron center from attack by Lewis bases, thus leaving it coordinatively unsaturated in the presence of fluoride ions.<sup>[26]</sup> Therefore, the electronics of the aromatic borepin nucleus do not preclude the use of the vacant boron p orbital in the context of Lewis basic sensing schemes unless the receptor incorporates some steric bulk.

The chloride “handles” were included at positions *para* to the boron in **1d** and **1e** (specifically where R<sup>1</sup> and/or R<sup>2</sup> are chlorides) because of their known reactivity under a variety of nickel- and palladium-catalyzed processes. For example, the chlorinated benzaldehyde **5b** was treated with phosphonium salt **4a** under the same Wittig-type conditions to prepare monochloro stilbene **2b** that was further reacted to form DBB **1d**, while both chlorinated units **4b** and **5b** were employed in the synthesis of **1e** under the same set of reactions. In principle, any of the aryl protons of **4** and **5** could be replaced with other substituents. The use of the Mes\* group was again required to impart robustness under ambient conditions.

DBBs with extended  $\pi$  conjugation were prepared from chlorides **1d** and **1e** by common cross-coupling procedures, thus illustrating the robustness of the protected DBB core. The homodimerization of **1d** that led to **7** was effected using a



nickel catalyst (with stoichiometric zinc reductant).<sup>[28,29]</sup> Kumada-type couplings of aryl Grignard reagents onto **1e** using [Ni(dppp)<sub>2</sub>Cl<sub>2</sub>] led to the aryl coupled products **8a–b**. As with the parent DBB, **7** and **8** were stable under ambient conditions and could be chromatographed with no apparent decomposition. Although treatment of the DBBs with molecular bromine led to decomposition, the dimer **7** did not react with *n*BuLi and even withstood an oxidative workup with aqueous hydrogen peroxide. We were unable to install other  $\pi$ -electron groups onto **1e** by using palladium-catalysts, and we could not install nonphenyl groups with nickel catalysts (e.g., with vinyl or ethynyl Grignard reagents). In some cases, clear dehalogenation of the DBB **1e** was observed, thus suggesting that the oxidative insertion was viable on the deactivated aryl chlorides and that future target-specific chemistry will be successful after reaction and substrate fine-tuning. The kinetic stability afforded by the Mes\* group will greatly facilitate future studies of this new electronic structure in the context of both small molecules and chemically synthesized polymeric materials that can be conceived from the functionalizable DBB cores.

The vacant p orbitals on boron can participate in extending the conjugation pathways in  $\pi$ -electron materials. Therefore, it was unusual to find that **7**, **8a**, and **8b** had quite similar optical properties (Table 1, Figure 1a,c). This finding can be rationalized by the presence of a node that is located at the site of aryl attachment in these molecules, and that localized the highest occupied molecular orbital (HOMO) wavefunc-

**Table 1:** Optical and electrochemical properties of functionalized borepin-containing  $\pi$ -electron molecules.

| Compound   | Abs <sup>[a]</sup><br>$\lambda_{\text{max}}$ [nm]<br>(log $\epsilon$ ) | PL<br>$\lambda_{\text{max}}$ [nm]<br>( $\Phi_F$ [%]) | $E_{1/2}(1)$ [V] | $E_{1/2}(2)$ [V]    |
|------------|--|--|------------------|---------------------|
| <b>1c</b>  | 358 (3.56)   | 384 (36)   | −2.54            | n.a. <sup>[b]</sup> |
| <b>7</b>   | 379 (3.43)   | 404 (58)   | −1.97            | −2.20               |
| <b>8a</b>  | 382 (2.97)   | 396 (23)   | −2.24            | n.a.                |
| <b>8b</b>  | 380 (3.55)   | 395 (38)   | −2.23            | n.a.                |
| <b>12a</b> | 439 (3.52)   | 456 (73)   | −1.89            | −2.59               |
| <b>13a</b> | 442 (3.33)   | 459 (56)   | −1.87            | −2.48               |
| <b>13b</b> | 438 (3.36)   | 459 (50)   | −1.88            | −2.46               |

[a] Lowest-energy  $\lambda_{\text{max}}$ . Full spectra and experimental details below and in the Supporting Information. [b] n.a. = not applicable.

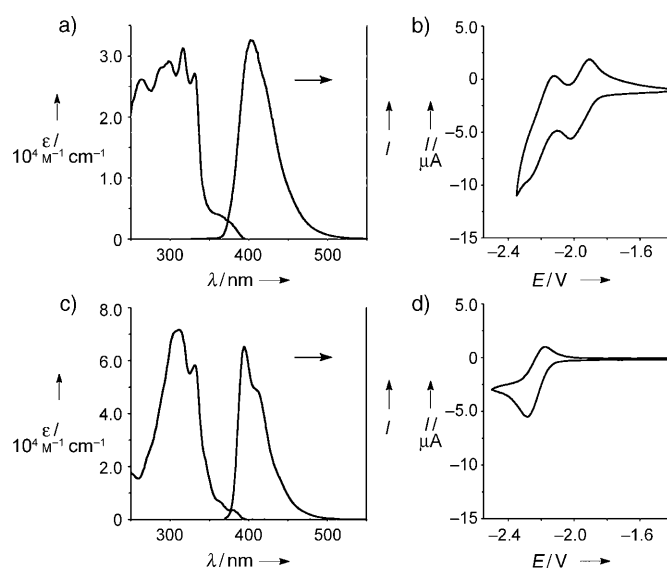
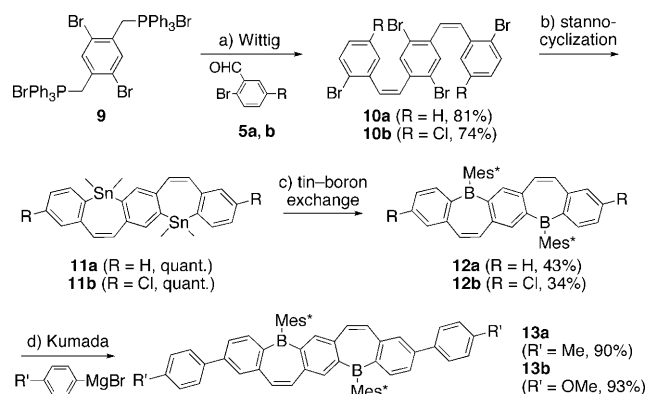


**Figure 1.** UV/Vis and photoluminescence (PL; a,c), and cyclic voltammetry (b,d) data for **7** (top) and **8b** (bottom). UV/Vis and PL spectra were acquired in CHCl<sub>3</sub> at room temperature, with an excitation at 317 (a) and 365 nm (b). CVs were acquired from 2.5 mM solutions of analyte in 0.1 M *n*Bu<sub>4</sub>NPF<sub>6</sub>/THF and are reported relative to Ag/Ag<sup>+</sup>.

tion on the DBB core, with only slight spreading onto the substituents in the lowest unoccupied molecular orbital (LUMO).<sup>[27]</sup> Both **7**, **8a**, and **8b** had their lowest-energy absorptions around 380 nm with photoluminescence maxima at approximately 400 nm. On the other hand, the more electron deficient DBB substituent of **7** led to a dramatic difference in cyclic voltammetry (CV) compared to **8a** and **8b**, showing less negative first (and second) reduction potentials ( $E_{1/2}$ s at −1.97 and −2.20 V for **7** vs. −2.24 V for **8a**, Figure 1 b,d). This result indicates that, despite the orbital wavefunction nodes at the site of aryl–aryl union, substantial communication, which influences the boron redox chemistry, still exists among the boron redox-active centers within the dimeric structure of **7**. This observation will be important for future work on electronic devices that often requires tuning the HOMO and LUMO levels relative to vacuum to facilitate charge injection as opposed to exploiting differences in optical bandgaps.

The general synthetic approach was applied to even larger fused polycyclic aromatics (Scheme 2). The bis(phosphonium) salt **9**<sup>[30]</sup> was subjected to a double-Wittig olefination



**Scheme 2.** Synthesis and diversification of pentacyclic borepins. Reagents and conditions: a) KOtBu, THF, 0 °C → RT; b) sBuLi, TMEDA, Me<sub>2</sub>SnCl<sub>2</sub>, THF, −78 °C → RT; c) BCl<sub>3</sub>, Mes\*Li, PhMe, −78 °C → RT; d) [Ni(dppp)<sub>2</sub>Cl<sub>2</sub>] (dppp = 1,3-bis(diphenylphosphino)propane), THF, 50 °C.

with bromobenzaldehyde **5a** to yield tetrabromide **10a**. Tetralithiation of **10a** followed by double stannocyclization led to **11a**. A double tin–boron exchange with BCl<sub>3</sub> generated a bis(chloride) intermediate that ultimately produced the fused pentacyclic aromatic **12a** when treated with Mes\*Li in situ. The structure of **12a** is fundamentally different from the DBB core as it now contains a *para*-phenylene diborane core,<sup>[31]</sup> that is, a central benzene core fused with two borepin rings. Like the *B*-Mes\* DBBs, **12a** could be handled under ambient conditions with no obvious decomposition. By using the same strategy as for **1e**, chlorides were installed *para* to the boron centers of **12b** and successfully underwent transformation under nickel catalysis to provide stable aryl-substituted compounds **13a** and **13b**. These compounds were thermally robust: **13a** showed no signs of decomposition after heating at 130 °C for 30 min, and the low-energy spectral signatures associated with the tricoordinate boron-based heteroaromatic were still observed after heating a sample over 250 °C in a melting-point apparatus.

Figure 2 shows some of the key characterization data for the unfunctionalized ring system **12a**. Like the profiles of the smaller DBB and other common polycyclic aromatics, the absorption profile of **12a** showed a low-energy feature at 439 nm with low oscillator strength attributed to intramolecular charge transfer along with much more intense absorptions at higher energy, including some with strong vibronic coupling around 375 nm (Figure 2a). The photoluminescence observed at 456 nm was fairly intense, with a quantum yield ( $\Phi_F$ ) of 73% relative to quinine sulfate. The cathodic CV indicated two reversible reduction steps with  $E_{1/2}$  values of −1.89 and −2.59 V (Figure 2b), both of which were much less negative than those found for standard triarylboranes.<sup>[31]</sup> As reported above, the spacing between the two cathodic processes for **7** ( $\Delta E_{1/2}$ ) was 230 mV while that for **12a** was even larger ( $\Delta E_{1/2}$  = 700 mV). This observation is consistent with the boron centers being separated formally by an

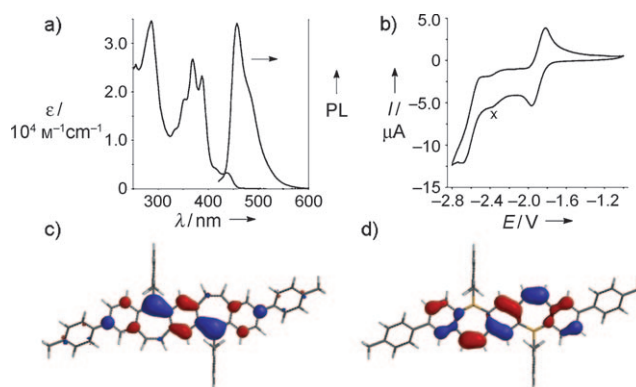


**Figure 2.** UV/Vis, photoluminescence (a) and cyclic voltammetry (b) data for **12a**. UV/Vis and PL were acquired in CHCl<sub>3</sub> at room temperature, with excitation at 415 nm. See Figure 1 for CV condition. The X in (b) denotes a background response from the electrolyte. DFT (B3LYP/6-31G\*) calculations depicting the LUMO (c) and HOMO (d) wavefunctions for **13a**.

intervening phenyl group in **12a** and a biphenyl unit in **7**. The smaller  $\Delta E_{1/2}$  value for **7** could also be due to Coulombic effects that place electronically isolated radical anions at a greater distance than for **12a**, but it is important to note that the initial  $E_{1/2}$  for dimer **7** is almost 600 mV less negative than that for **1c**, thus indicating some extent of existing electronic communication that facilitates the reduction. Importantly, all cathodic processes observed for these molecules were reversible, thus suggesting that they may be used as electron-accepting organic semiconducting materials.

Unexpectedly, the attachment of the aryl groups did not dramatically affect the photophysical or electrochemical behavior relative to the parent compound **12a**. We carried out DFT (B3LYP/6-31G\*) calculations for the LUMO and HOMO of **13a** (but using *B*-2,6-dimethylphenyl rather than *B*-Mes\*, Figure 2c,d). The HOMO level is localized on the polycyclic aromatic core with a node at the site of tolyl attachment, and the LUMO has very minimal delocalization onto the aryl substituents. We anticipate more electronic influence to be exerted by substituents placed elsewhere onto the fused core, as determined by the choice of benzaldehyde precursors **5** that ultimately determines the site for functionalization.

The X-ray structure of a single crystal (grown from a mixture of THF, CH<sub>2</sub>Cl<sub>2</sub>, and water) verified the molecular connectivity (Figure 3a) and revealed important packing-induced distortions within the pentacyclic core (deviation from planarity  $\approx$  14°; Figure 3b).<sup>[32]</sup> As the DFT calculations indicate a planar pentacyclic aromatic core, we attribute these deviations to crystal-packing influences as well as deformations imposed by the Mes\* group; these deviations are also spectroscopically apparent for the DBB **1c**. The structural metrics of the borepin core were consistent with other borepin fragments reported previously,<sup>[24]</sup> and the NICS(1)<sup>[33]</sup> calculated for the borepin ring of **12a** (−1.65) indicated very weak local aromaticity or perhaps even nonaromatic behavior. Although small in absolute value, it is comparable to that calculated in our labs for the weakly aromatic *B*-phenylborepin (−5.75), thus indicating that the

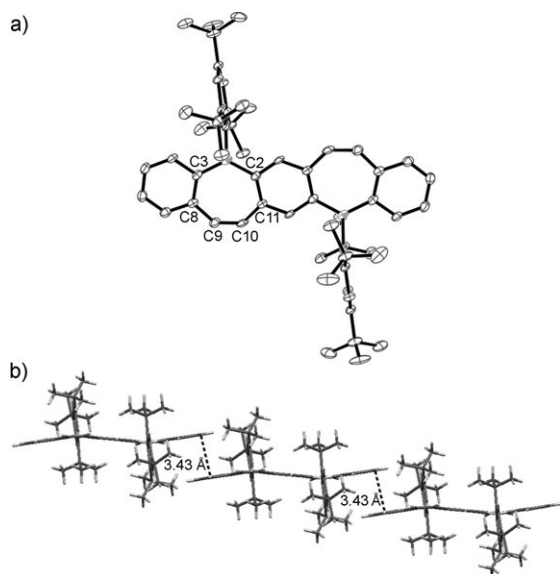


**Figure 3.** Displacement ellipsoid plot (50% probability level) of **12a** at 110(2) K (a) and an extended packing motif (b) revealing face-to-face aromatic contacts spaced at 3.43 Å. Selected bond lengths [Å]: B1–C2 1.573(3), B1–C3 1.570(3), C3–C8 1.423(3), C8–C9 1.452(3), C9–C10 1.341(3), C10–C11 1.452(3), C2–C11 1.421(3).

inherent borepin aromaticity is not dramatically perturbed by extended ring fusion. Finally, the Mes\* groups frustrated tight packing leaves substantial void spaces within the crystal lattice.<sup>[27]</sup> These voids are occupied by a mixture of disordered solvent molecules (CH<sub>2</sub>Cl<sub>2</sub> and THF), and their contributions were subsequently removed for the last stage of refinement using the SQUEEZE program.<sup>[34]</sup> Face-to-face  $\pi$  stacking with a distance of 3.43 Å was evident at the periphery of the pentacyclic fragment.

We have reported a synthetic approach that enables the construction of functionalizable borepin-based polycyclic aromatic compounds. The synthetic approach was extended to pentacyclic aromatic compounds that bear two fused borepin rings; these compounds are analogous to pentacyclic aromatic hydrocarbons such as pentacene or dibenz-[a,h]anthracene, or can act as model systems for extended ladder polymers.<sup>[35]</sup> The bulky *B*-Mes\* moiety shields the sensitive boron center from undesired reactivity, thus allowing for standard synthetic manipulation and isolation under ambient conditions. We are currently exploring prospects for an expanded cross-coupling repertoire among new substrates with different substitution patterns about the borepin scaffolds and the evaluation of the products as new electronic materials.

## Experimental Section

**Synthesis:** All synthetic manipulations were conducted using standard Schlenk air-free techniques. Synthetic procedures and detailed molecular characterization data can be found in the Supporting Information.

**Photophysical studies:** Spectroscopic measurements were conducted in CHCl<sub>3</sub> at room temperature. UV/Vis absorption spectra

were recorded on a Varian Cary 50 Bio UV/Visible spectrophotometer. Photoluminescence spectra were recorded on a Photon Technologies QuantaMaster 4 fluorometer with a 75 W Xenon lamp, maintaining optical densities below 0.05. Quantum yields were determined relative to quinine sulfate in 0.1N H<sub>2</sub>SO<sub>4</sub> (55 %).

**Electrochemistry:** Cyclic voltammetry was performed in a one-chamber, three-electrode cell using PARSTAT 2273 and Autolab PGSTAT 302 potentiostats. A 2 mm<sup>2</sup> Pt button electrode was used as the working electrode with a platinum wire counter electrode relative to a quasi-internal Ag wire reference electrode submersed in 0.01M AgNO<sub>3</sub>/0.1M *n*Bu<sub>4</sub>NPF<sub>6</sub> in anhydrous acetonitrile (obtained from BioAnalytical Systems, West Lafayette, IN, USA). Measurements recorded on millimolar analyte concentrations in 0.1M *n*Bu<sub>4</sub>NPF<sub>6</sub> electrolyte solutions (in THF) recorded at a scan rate of 100 mV s<sup>−1</sup>. Potentials are reported relative to the Ag/Ag<sup>+</sup> couple (ferrocene/ferrocenyl (Fc/Fc<sup>+</sup>) = 205 mV).

**Computational studies:** Molecular orbital calculations were performed at the DFT level (B3LYP/6-31G\*) on equilibrium geometries using Spartan'04 (Wavefunction Inc., Irvine, CA). NICS calculations were performed using Gaussian 03 using the GIAO method (B3LYP/6-31G\*).<sup>[36]</sup>

Received: January 23, 2010

Revised: March 29, 2010

Published online: May 7, 2010

**Keywords:** annulation · aromaticity · boron · conjugation · cross-coupling

- [1] J. C. Collings, S. Y. Poon, C. Le Droumaguet, M. Charlot, C. Katan, L. O. Palsson, A. Beeby, J. A. Mosely, H. M. Kaiser, D. Kaufmann, W. Y. Wong, M. Blanchard-Desce, T. B. Marder, *Chem. Eur. J.* **2009**, *15*, 198–208.
- [2] H. Li, F. Jäkle, *Angew. Chem.* **2009**, *121*, 2349–2352; *Angew. Chem. Int. Ed.* **2009**, *48*, 2313–2316.
- [3] N. Matsumi, M. Miyata, Y. Chujo, *Macromolecules* **1999**, *32*, 4467–4469.
- [4] A. Wakamiya, K. Mori, S. Yamaguchi, *Angew. Chem.* **2007**, *119*, 4351–4354; *Angew. Chem. Int. Ed.* **2007**, *46*, 4273–4276.
- [5] T. K. Wood, W. E. Piers, B. A. Keay, M. Parvez, *Angew. Chem.* **2009**, *121*, 4069–4072; *Angew. Chem. Int. Ed.* **2009**, *48*, 4009–4012.
- [6] G. Zhou, M. Baumgarten, K. Müllen, *J. Am. Chem. Soc.* **2008**, *130*, 12477–12484.
- [7] A. Lorbach, M. Bolte, H. Y. Li, H. W. Lerner, M. C. Holthausen, F. Jäkle, M. Wagner, *Angew. Chem.* **2009**, *121*, 4654–4658; *Angew. Chem. Int. Ed.* **2009**, *48*, 4584–4588.
- [8] T. W. Hudnall, F. P. Gabbaï, *J. Am. Chem. Soc.* **2007**, *129*, 11978–11986.
- [9] S. Yamaguchi, S. Akiyama, K. Tamao, *J. Am. Chem. Soc.* **2001**, *123*, 11372–11375.
- [10] B. Y. Lee, S. J. Wang, M. Putzer, G. P. Bartholomew, X. H. Bu, G. C. Bazan, *J. Am. Chem. Soc.* **2000**, *122*, 3969–3970.
- [11] A. J. Ashe, J. W. Kampf, C. M. Kausch, H. Konishi, M. O. Kristen, J. Kroker, *Organometallics* **1990**, *9*, 2944–2948.
- [12] D. A. Hoic, W. M. Davis, G. C. Fu, *J. Am. Chem. Soc.* **1995**, *117*, 8480–8481.
- [13] J. M. Schulman, R. L. Disch, *Organometallics* **2000**, *19*, 2932–2936.
- [14] G. Subramanian, P. von R. Schleyer, H. J. Jiao, *Organometallics* **1997**, *16*, 2362–2369.
- [15] A. J. V. Marwitz, M. H. Matus, L. N. Zakharov, D. A. Dixon, S. Y. Liu, *Angew. Chem.* **2009**, *121*, 991–995; *Angew. Chem. Int. Ed.* **2009**, *48*, 973–977.



- [16] M. J. D. Bosdet, W. E. Piers, T. S. Sorensen, M. Parvez, *Angew. Chem.* **2007**, *119*, 5028–5031; *Angew. Chem. Int. Ed.* **2007**, *46*, 4940–4943.
- [17] N. Matsumi, K. Naka, Y. Chujo, *J. Am. Chem. Soc.* **1998**, *120*, 10776–10777.
- [18] C. H. Zhao, A. Wakamiya, Y. Inukai, S. Yamaguchi, *J. Am. Chem. Soc.* **2006**, *128*, 15934–15935.
- [19] H. Y. Li, A. Sundararaman, K. Venkatasubbaiah, F. Jäkle, *J. Am. Chem. Soc.* **2007**, *129*, 5792–5793.
- [20] S. Yamaguchi, T. Shirasaka, S. Akiyama, K. Tamao, *J. Am. Chem. Soc.* **2002**, *124*, 8816–8817.
- [21] A. Caruso, Jr., J. D. Tovar in *Proceedings of the 236th ACS National Meeting*, Philadelphia, **2008**.
- [22] L. G. Mercier, W. E. Piers, in *91st Canadian Chemistry Conference and Exhibition*, Edmonton, Canada, **2008**.
- [23] E. E. van Tamelen, G. Brieger, K. G. Untch, *Tetrahedron Lett.* **1960**, *1*, 14–15.
- [24] L. G. Mercier, W. E. Piers, M. Parvez, *Angew. Chem.* **2009**, *121*, 6224–6227; *Angew. Chem. Int. Ed.* **2009**, *48*, 6108–6111.
- [25] E. C. Dunne, E. J. Coyne, P. B. Crowley, D. G. Gilheany, *Tetrahedron Lett.* **2002**, *43*, 2449–2453.
- [26] A. Wakamiya, K. Mishima, K. Ekawa, S. Yamaguchi, *Chem. Commun.* **2008**, 579–581.
- [27] See the Supporting Information.
- [28] I. Colon, D. R. Kelsey, *J. Org. Chem.* **1986**, *51*, 2627–2637.
- [29] J. L. Reddinger, J. R. Reynolds, *Macromolecules* **1997**, *30*, 479–481.
- [30] M. C. Bonifacio, C. R. Robertson, J. Y. Jung, B. T. King, *J. Org. Chem.* **2005**, *70*, 8522–8526.
- [31] W. Kaim, A. Schulz, *Angew. Chem.* **1984**, *96*, 611–612; *Angew. Chem. Int. Ed. Engl.* **1984**, *23*, 615–616.
- [32]  $C_{58}H_{72}B_2$ ;  $M_r = 790.78$ ; pale yellow plate;  $0.41 \times 0.26 \times 0.08 \text{ mm}^3$ ; triclinic;  $P\bar{1}$  (no. 2),  $a = 9.8252(3)$ ,  $b = 10.1043(2)$ ,  $c = 13.8222(4) \text{ \AA}$ ;  $\alpha = 99.775(2)$ ,  $\beta = 100.226(2)$ ,  $\gamma = 92.362(2)$ ;  $V = 1327.21(6) \text{ \AA}^3$ ;  $Z = 1$ ;  $D_x = 0.989 \text{ g cm}^{-3}$ ;  $Mo_{K\alpha}$  radiation ( $\lambda = 0.71073 \text{ \AA}$ );  $T = 110(2) \text{ K}$ ;  $\mu = 0.055 \text{ mm}^{-1}$ ; abs. corr. range: 0.984–0.997. Reported data excludes solvent contributions. 13951 reflections were measured up to a resolution of  $(\sin\theta/\lambda)_{\text{max}} = 0.59 \text{ \AA}^{-1}$ . 4664 reflections were unique ( $R_{\text{int}} = 0.0548$ ), of which 2920 were observed [ $I > 2\sigma(I)$ ]. 290 parameters were refined using 110 restraints.  $R1/wR2$  [ $I > 2\sigma(I)$ ]: 0.0571/0.1480.  $R1/wR2$  [all data]: 0.0944/0.1579.  $S = 0.959$ . Residual electron density found between  $-0.25$  and  $0.23 \text{ e \AA}^{-3}$ . CCDC 762997 contains the supplementary crystallographic data for this paper. These data can be obtained free of charge from The Cambridge Crystallographic Data Centre via [www.ccdc.cam.ac.uk/data\\_request/cif](http://www.ccdc.cam.ac.uk/data_request/cif).
- [33] NICS(1) refers to the shift of an arbitrary “ghost atom” located  $1 \text{ \AA}$  above the center of the ring, see: P. von R. Schleyer, C. Maerker, A. Dransfeld, H. J. Jiao, N. J. R. V. Hommes, *J. Am. Chem. Soc.* **1996**, *118*, 6317–6318.
- [34] A. L. Spek, *J. Appl. Crystallogr.* **2003**, *36*, 7–13.
- [35] S. Yamaguchi, C. H. Xu, T. Okamoto, *Pure Appl. Chem.* **2006**, *78*, 721–730.
- [36] Gaussian03, Revision C.01, M. J. Frisch et al., Gaussian, Inc., Wallingford, CT, **2004**.